

УДК 537.312:538.911'956

Doi: 10.31772/2712-8970-2023-24-3-613-620

---

**Для цитирования:** Харьков А. М., Ситников М. Н., Аплеснин С. С. Магнитоимпеданс в нестехиометрическом сульфиде марганца // Сибирский аэрокосмический журнал. 2023. Т. 24, № 3. С. 613–620. Doi: 10.31772/2712-8970-2023-24-3-613-620.

**For citation:** Kharkov A. M., Sitnikov M. N., Aplesnin S. S. [Magnetic impedance in nonstochiometric manganese sulfide]. *Siberian Aerospace Journal*. 2023, Vol. 24, No. 3, P. 613–620. Doi: 10.31772/2712-8970-2023-24-3-613-620.

---

## Magnetic impedance in nonstochiometric manganese sulfide

A. M. Kharkov, M. N. Sitnikov, S. S. Aplesnin

Reshetnev Siberian State University of Science and Technology  
31, Krasnoyarskii Rabochii prospekt, Krasnoyarsk, 660037, Russian Federation  
E-mail: kharkanton@mail.ru

*The role of defects on the dynamic characteristics of manganese sulfide is studied by impedance spectroscopy in the frequency range  $10^2$ – $10^6$  Hz and temperatures 80–500 K. Nonstoichiometry plays an important role in the formation of new transport and magnetic properties, as it leads to electrically inhomogeneous states. The phase composition and crystal structure of nonstochiometric manganese sulfide were studied on a DRON-3 X-ray unit using  $CuK\alpha$  – radiation at room temperature. According to X-ray diffraction analysis, the synthesized compound is single-phase and has a  $NaCl$ -type cubic lattice. From the frequency dependences of the impedance components measured in the absence of a field and in a magnetic field, the relaxation time of the current carriers in the Debye model is found. A sharp decrease in the relaxation time and its correlation with conductivity were found. The contribution to the impedance of the active and reactive parts of the impedance at frequencies below and above the relaxation time is established. The capacitance from the impedance hodograph in the equivalent circuit model is determined. In defective manganese sulfide, the temperature-dependent impedance has an activation character. The activation energy is determined in the range 250–500 K, which is attributed to the excitation energy of lattice polarons. The effect of a magnetic field on the dynamic characteristics of current carriers was studied as a result of a change in the impedance components in a magnetic field at fixed temperatures. The impedance increases in a magnetic field and reaches a maximum in the temperature range of charge ordering of vacancies. An increase in the impedance in a magnetic field is explained by a decrease in the diagonal component of the permittivity in a magnetic field in an electrically inhomogeneous medium. The experimental data are explained in the Debye model.*

*Keywords:* semiconductors, impedance, magnetoimpedance, Debye model.

## Магнитоимпеданс в нестехиометрическом сульфиде марганца

А. М. Харьков, М. Н. Ситников, С. С. Аплеснин

Сибирский государственный университет науки и технологий имени академика М. Ф. Решетнева  
Российская Федерация, 660037, г. Красноярск, просп. им. газ. «Красноярский Рабочий», 31  
E-mail: kharkanton@mail.ru

*Исследуется роль дефектов на динамические характеристики сульфида марганца методом импедансной спектроскопии в интервале частот  $10^2$ – $10^6$  Гц и температур 80–500 К. Нестехиометрия играет важную роль в формировании новых транспортных и магнитных свойств, так как приводит к электрически неоднородным состояниям. Фазовый состав и кристаллическая структура нестехиометрического сульфида марганца исследовались на рентгеновской установке ДРОН-3*

с использованием  $\text{CuK}_\alpha$  – излучения при комнатной температуре. Согласно рентгеноструктурному анализу, синтезированные соединения являются однофазными и имеют кубическую решетку типа  $\text{NaCl}$ . Из частотных зависимостей компонент импеданса, измеренных без поля и в магнитном поле, найдено время релаксации носителей тока в модели Дебая. Обнаружено резкое уменьшение времени релаксации и ее корреляция с проводимостью. Установлен вклад в импеданс активной и реактивной частей импеданса на частотах меньше и больше времени релаксации. Определена емкость из голографа импеданса в модели эквивалентных схем. В дефектном сульфиде марганца импеданс от температуры имеет активационный характер. Определена энергия активации в интервале 250–500 К, которая приписывается энергии возбуждения решеточных поляронов. Влияние магнитного поля на динамические характеристики носителей тока исследовалось в результате изменения компонент импеданса в магнитном поле при фиксированных температурах. Импеданс увеличивается в магнитном поле и достигает максимума в области температуры зарядового упорядочения вакансий. Увеличение импеданса в магнитном поле объясняется уменьшением диагональной компоненты диэлектрической проницаемости в магнитном поле в электрически неоднородной среде. Экспериментальные данные объясняются в модели Дебая.

*Ключевые слова:* полупроводники, импеданс, магнитоимпеданс, модель Дебая.

## Introduction

The development of electronic devices that can function in extreme conditions, such as small spacecraft, where the ambient temperature varies from 200 до 400 K, is an urgent task. That's why spintronics attracts attention [1–4]. The control of transport characteristics in semiconductors under the influence of an external magnetic field is of interest from both a fundamental and a practical point of view [5–8]. In electrically inhomogeneous semiconductors, the transport characteristics at direct and alternating current can be qualitatively different [9]. This is due to the radius of inhomogeneity and the relaxation time of the current carriers, which is determined by the interaction with magnetic and elastic subsystems. Electrical inhomogeneity can be controlled by electronic doping, concentration, and temperature.

For example, in manganites, during uninsulated substitution, transitions related to orbital, charge, and magnetic ordering were found [10–13]. In iron oxides  $\text{Fe}_3\text{O}_4$  above the Verwey temperature, an electron nematic with a correlation radius of 5–8 nm was found. The Verwey transition is associated with competition of charge and structural order as a result of electron-phonon interaction [14]. It is possible to obtain charge ordering in manganese sulfide, where the current carriers are lattice polarons due to non-stoichiometry. Manganese sulfide is a magnetic semiconductor with a Néel temperature of 150 K, a gap in the electron excitation spectrum of 3 eV [15; 16]. Degeneracy in the region of charge ordering is removed by the magnetic field, i.e., the topology of the electrically inhomogeneous state changes in the magnetic field, which leads to a change in the frequency dependence of the dielectric constant in the magnetic field, and the prerequisites for magnetoimpedance are created.

The purpose of the work is to establish the magnetic field influence of the on the AC resistance and impedance components in the non-stoichiometric  $\text{Mn}_{0.9}\text{S}$  sample.

## Materials and methods

The phase composition and crystal structure of the  $\text{Mn}_{0.9}\text{S}$  sample were studied on a DRON-3 X-ray installation using  $\text{CuK}_\alpha$  radiation at room temperature. According to X-ray diffraction analysis, the synthesized compounds are single-phase and have a  $\text{NaCl}$ -type cubic lattice, as in the original manganese sulfide [15].

Impedance, active and reactive parts of the impedance were measured on an AM-3028 component analyzer in the frequency range  $\omega = 10^2\text{--}10^6$  Hz at temperatures of 77–500 K, the amplitude of the alternating voltage was 1 V. To calculate the impedance spectra, ZView software (Scribner Associates Inc.) was used.

## Results and discussion

The inhomogeneous electrical state and the formation of a space charge can be established from impedance spectroscopy [17]. From the impedance we will establish the dynamic characteristics of current carriers, the relaxation time, and the mechanism of dissipation of current carriers will be revealed from the impedance. Figure 1 shows the frequency dependences of the impedance components without a field and in a magnetic field, which are well described in the Debye model [18]:

$$\operatorname{Re} Z(\omega) = \frac{A}{1 + (\omega\tau)^2}; \quad \operatorname{Im} Z(\omega) = \frac{B\omega\tau}{1 + (\omega\tau)^2}, \quad (1)$$

where  $\tau$  is the relaxation time of the current carriers, A and B parameters.

The relaxation time decreases by a factor of five when heated and reaches a minimum at 450 K (inset in Fig. 1,*b*). At this temperature, the conductivity reaches its maximum.

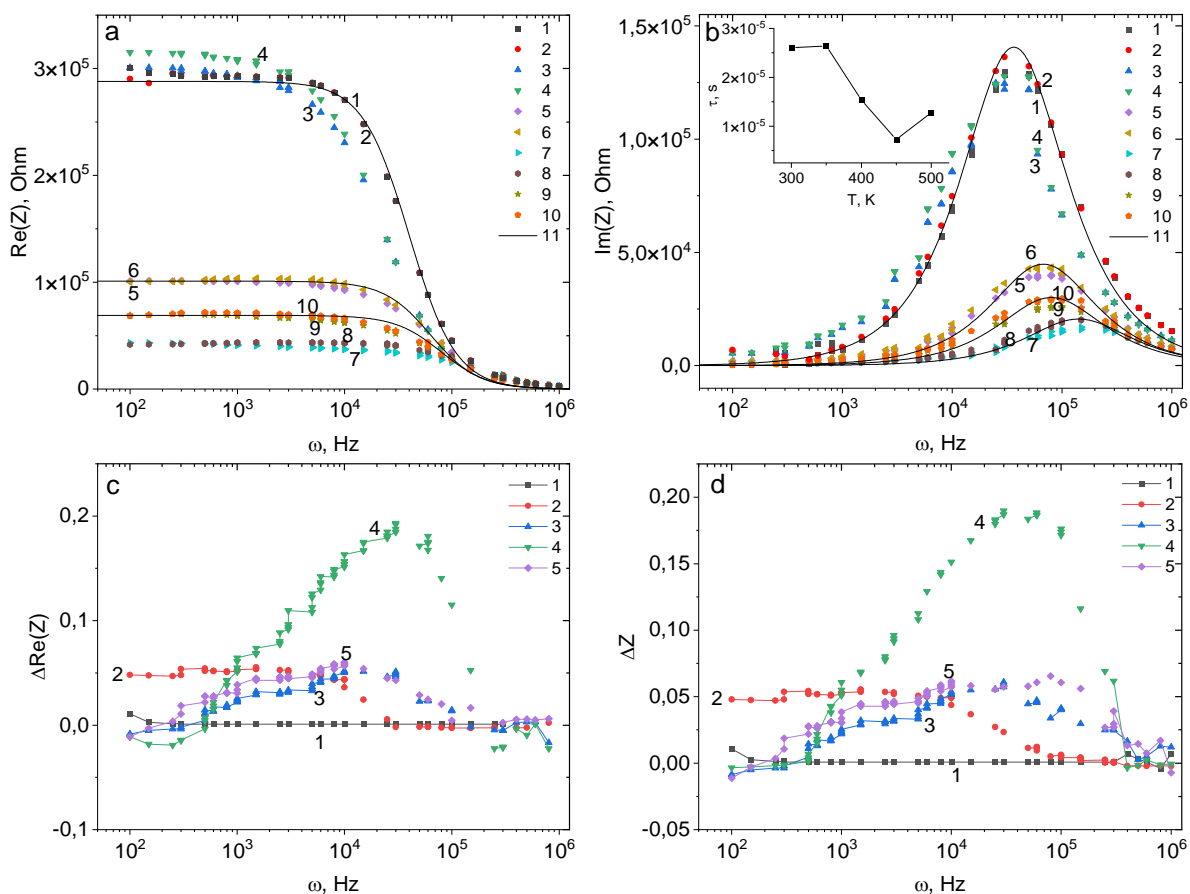


Рис. 1. Частотные зависимости действительной (*a*) и мнимой (*b*) частей импеданса для образца  $Mn_{0.9}S$  без поля  $H = 0$  (1, 3, 5, 7, 9) и в магнитном поле  $H = 12$  кЭ (2, 4, 6, 8, 10) при температурах  $T = 300$  К (1, 2), 350 К (3, 4), 400 К (5, 6), 450 К (7, 8), 500 К (9, 10). Подгоночные функции (11). Вставка: температурная зависимость времени релаксации  $\tau$ . Частотные зависимости магнитоимпеданса для действительной его части (*c*) и магнитоимпеданса  $\Delta Z$  (*d*) в магнитном поле  $H = 12$  кЭ при температурах  $T = 300$  К (1), 350 К (2), 400 К (3), 450 К (4), 500 К (5) для образца  $Mn_{0.9}S$

Fig. 1. Frequency dependences of the real (*a*) and imaginary (*b*) parts of the impedance for the  $Mn_{0.9}S$  sample without a field  $H = 0$  (1, 3, 5, 7, 9) and in a magnetic field  $H = 12$  kOe (2, 4, 6, 8, 10) at temperatures  $T = 300$  K (1, 2), 350 K (3, 4), 400 K (5, 6), 450 K (7, 8), 500 K (9, 10). Fitting functions (11). Insert: temperature dependence of relaxation time  $\tau$ . Frequency dependences of the magnetoimpedance for its real part (*c*) and magnetoimpedance  $\Delta Z$  (*d*) in a magnetic field  $H = 12$  kOe at temperatures  $T = 300$  K (1), 350 K (2), 400 K (3), 450 K (4), 500 K (5) for the  $Mn_{0.9}S$  sample

The magnetic field influence on the dynamic characteristics of current carriers was studied as a result of changes in impedance components in a magnetic field at fixed temperatures:

$$\Delta R = \text{Re}(Z(H, \omega)) - \text{Re}(Z(H = 0, \omega)) / \text{Re}(Z(H = 0, \omega));$$

$$\Delta Z = (Z(H, \omega) - Z(H = 0, \omega)) / Z(H = 0, \omega)) \quad (2)$$

The impedance increases in a magnetic field and reaches a maximum in the temperature of charge ordering of vacancies (Fig. 1 d). The increase in  $\text{Re}(Z)$  in a magnetic field is caused by a decrease in the diagonal component of the dielectric constant in the magnetic field (Fig. 1, c). Conductivity is proportional to dielectric constant  $\sigma = i\omega\epsilon$ . In an electrically inhomogeneous medium, the longitudinal component of the dielectric constant looks like [19]:

$$\text{Re}[\epsilon_{xx}(\omega)] = \frac{\epsilon(1 - \beta^2 + (\omega\tau)^2(1 + \beta^2)^2)}{1 + (\omega\tau)^2(1 + \beta^2)^2}, \quad (3)$$

where  $\beta = \mu H$ ;  $\mu$  is mobility;  $\tau = \epsilon/\sigma$ .

The presence of space charge, which is created by defects, can be assessed from the impedance hodograph. Figure 2 shows the impedance hodographs of  $\text{Mn}_{0.9}\text{S}$ . In the equivalent circuit model the hodograph is described by series resistance  $R_1$  and parallel components  $R_2$  and  $C$  (Fig. 2). The resistance  $R_1$  is an order of magnitude smaller than  $R_2$  and the capacitance is about  $C \sim 100 \text{ pF}$ .

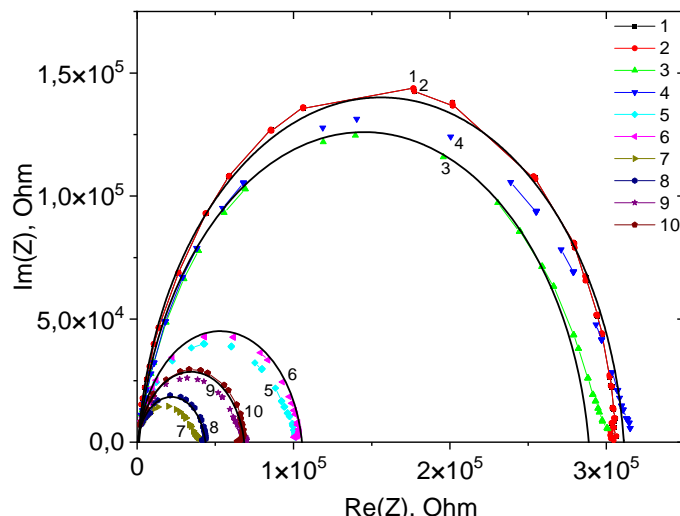


Рис. 2. Годографы импеданса для образца  $\text{Mn}_{0.9}\text{S}$  в нулевом магнитном поле (1, 3, 5, 7, 9) и в магнитном поле  $H = 12 \text{ кЭ}$  (2, 4, 6, 8, 10) при температурах  $T = 300 \text{ K}$  (1, 2),  $350 \text{ K}$  (3, 4),  $400 \text{ K}$  (5, 6),  $450 \text{ K}$  (7, 8),  $500 \text{ K}$  (9, 10)

Fig. 2. Impedance hodographs for the  $\text{Mn}_{0.9}\text{S}$  sample in a zero magnetic field (1, 3, 5, 7, 9) and in a magnetic field  $H = 12 \text{ kOe}$  (2, 4, 6, 8, 10) at temperatures  $T = 300 \text{ K}$  (1, 2),  $350 \text{ K}$  (3, 4),  $400 \text{ K}$  (5, 6),  $450 \text{ K}$  (7, 8),  $500 \text{ K}$  (9, 10)

Impedance is determined by the active part  $R$  and the reactive ( $\omega L - 1/\omega C$ ) part. Contributions to impedance depend on temperature. The temperature dependence of the impedance of  $\text{Mn}_{0.9}\text{S}$  is given in Fig. 3. At measurement times less than the relaxation time  $\tau < \tau_c$  up to 200 K, the impedance is due to the reactive part. Impurity charged defect states are shielded, and the capacitance is practically independent of temperature. Depolarization causes a slight increase in direct current resistance and increases the contribution to the impedance from the reactive part. When heated, the impedance decreases by 4–5 orders of magnitude above 200 K. The change in impedance with temperature has an activation character  $Z(T) = Z_0 \exp(\Delta E/kT)$  with activation energy  $\Delta E = 0.11 - 0.13 \text{ eV}$  in the range

250–500 K. This energy corresponds to the excitation energy of lattice polarons, which were observed in  $\text{La}_{0.9}\text{Sr}_{0.1}\text{MnO}_3$  manganites and are attributed to Jahn-Teller polarons [20–21].

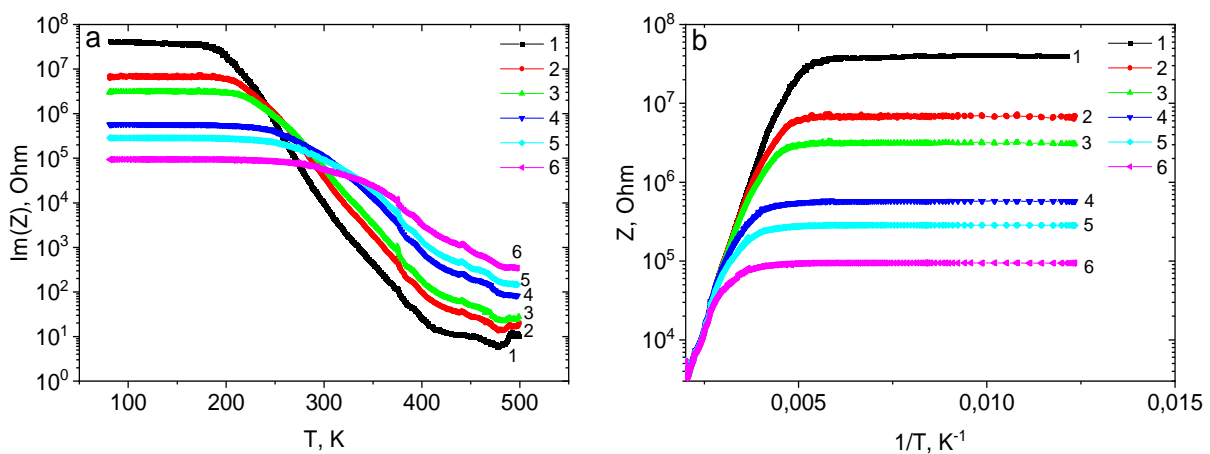


Рис. 3. Температурная зависимость мнимой части импеданса (a) и импеданса от обратной температуры (b)  $\omega = 1 \text{ кГц}$  (1),  $5 \text{ кГц}$  (2),  $10 \text{ кГц}$  (3),  $50 \text{ кГц}$  (4),  $100 \text{ кГц}$  (5),  $1000 \text{ кГц}$  (6) для образца  $\text{Mn}_{0.9}\text{S}$

Fig. 3. Temperature dependence of imaginary part of impedance (a) and impedance on inverse temperature (b)  $\omega = 1 \text{ kHz}$  (1),  $5 \text{ kHz}$  (2),  $10 \text{ kHz}$  (3),  $50 \text{ kHz}$  (4),  $100 \text{ kHz}$  (5),  $1000 \text{ kHz}$  (6) for the  $\text{Mn}_{0.9}\text{S}$  sample

### Conclusion

A comparison of the impedance component in manganese sulfide with defects in the manganese cationic system indicates the main contribution of electrical resistivity to the magnetoimpedance. The temperature of the maximum magnetic impedance and the relaxation time of current carriers are found. The impedance hodograph is described by a single RC circuit with series resistance, and the electrical conductivity is determined by the bulk properties of the crystallite. Defects in manganese sulfide  $\text{Mn}_{0.9}\text{S}$  cause a capacitive contribution to the impedance below 200 K. Depolarization of impurity centers at 200 K induces a maximum conductivity and a transition to the activation dependence of the impedance on temperature associated with lattice polarons. The temperature at which the minimum relaxation of current carriers causes a maximum of conductivity and an increase in impedance in the magnetic field has been found.

**Благодарности.** Работа поддержана Российским научным фондом, Правительством Красноярского края и проектом Красноярского научного фонда № 23-22-10016.

**Acknowledgments.** The work was supported by the Russian Medium Fund, the Government of the Krasnoyarsk Territory and the Krasnoyarsk Science Foundation project No. 23-22-10016.

### Библиографические ссылки

1. Epitaxial  $\text{BiFeO}_3$  multiferroic thin film heterostructures / J. Wang, J. B. Neaton, H. Zheng et al. // Science. 2003. Vol. 299. P. 1719.
2. Zvezdin A. K., Pyatakov A. P. Phase transitions and the giant magnetoelectric effect in multiferroics // Usp. Fiz. Nauk. 2004. Vol. 174, Is. 4. P. 465.

3. Multiferroics: Promising materials for microelectronics, spintronics, and sensor technique / A. K. Zvezdin, A. S. Logginov, G. A. Meshkov et al. // Bull. Russ. Acad. Sci. Phys. 2007. Vol. 71. P. 1561.
4. Апленчин С. С. Основы спинtronики // СПб. : Лань, 2022. 288 с.
5. Giant Magnetoresistance: Basic Concepts, Microstructure, Magnetic Interactions and Applications / I. Ennen, D. Kappe, T. Rempel et al. // Sensors. 2016. Vol. 16, Is. 6. P. 904.
6. Enhanced magnetoresistance in layered magnetic structures with antiferromagnetic interlayer exchange / G. Binasch, P. Grunberg, F. Saurenbach, W. Zinn // Phys. Rev. B. 1989. Vol. 39. P. 4828.
7. Aplesnin S. S., Romanova O. B., Yanushkevich K. I. Magnetoresistance effect in anion-substituted manganese chalcogenides // Phys. Stat. Sol. B Basic Research. 2015. Vol. 252, Is. 8. P. 1792.
8. Magnetoelectric and magnetoresistive properties of the  $\text{Ce}_x\text{Mn}_{1-x}\text{S}$  semiconductors / S. S. Aplesnin, M. N. Sitnikov, O. B. Romanova et al. // Phys. Stat. Sol. B Basic Research. 2016. Vol. 253, Is. 9. P. 1771.
9. Magnetoresistance and magnetoimpedance in holmium manganese sulfides / O. B. Romanova, S. S. Aplesnin, M. N. Sitnikov et al. // Appl. Phys. A. 2022. Vol. 128. P. 124.
10. Structural, magnetic, and dielectric properties of charge-order phases in manganite  $\text{La}(\text{Ca}_{0.8}\text{Sr}_{0.2})_2\text{Mn}_2\text{O}_7$  / J. H. Zhang, S. H. Zheng, Y. S. Tang et al. // J. Appl. Phys. 2020. Vol. 127. P. 104301.
11. Papavassiliou J. The Pinch Technique at Two Loops // Phys. Rev. Lett. 2000. Vol. 84. P. 2782.
12. Electronic phase separation in lanthanum manganites: Evidence from  $^{55}\text{Mn}$  NMR / G. Allodi, R. De Renzi, G. Guidi et al. // Phys. Rev. B. 1997. Vol. 56. P. 6036.
13. Liquidlike Spatial Distribution of Magnetic Droplets Revealed by Neutron Scattering in  $\text{La}_{1-x}\text{Ca}_x\text{MnO}_3$  / M. Hennion, F. Moussa, G. Biotteau et al. // Phys. Rev. Lett. 1998. Vol. 81. P. 1957.
14. Verwey transition as evolution from electronic nematicity to trimers via electron-phonon coupling / W. Wang, J. Li, Z. Liang et al. // Sci. Adv. 2023. Vol. 9. P. 8220.
15. Spin-dependent transport in  $\alpha$ -MnS single crystals / S. S. Aplesnin, L. I. Ryabinkina, G. M. Abramova et al. // Phys. Sol. St. 2004. Vol. 46, Is. 11. P. 2067.
16. Conductivity, weak ferromagnetism, and charge instability in an  $\alpha$ -MnS single crystal / S. S. Aplesnin, L. I. Ryabinkina, G. M. Abramova et al. // Phys. Rev. B. 2005. Vol. 71, Is. 12. P. 125204.
17. Electrochemical impedance spectroscopy / S. Wang, J. Zhang, O. Gharbi et al. // Nat. Rev. Meth. Prim. 2021. Vol. 1. P. 41.
18. Holm S. Time domain characterization of the Cole-Cole dielectric model // J. Electr. Bioimpedance. 2020. Vol. 11, Is. 1. P. 101.
19. Parish M. M., Littlewood P. B. Magnetocapacitance in Nonmagnetic Composite Media // Phys. Rev. Lett. 2008. Vol. 101. P. 166602.
20. Yang Y.-F., Held K. Localization of strongly correlated electrons as Jahn-Teller polarons in manganites // Phys. Rev. B. 2007. Vol. 76. P. 212401.
21. Magnetic-field-induced suppression of Jahn-Teller phonon bands in  $(\text{La}_{0.6}\text{Pr}_{0.4})_{0.7}\text{Ca}_{0.3}\text{MnO}_3$ : the mechanism of colossal magnetoresistance shown by Raman spectroscopy / S. Merten, O. Shapoval, B. Damaschke et al. // Sci. Rep. 2019. Vol. 9. P. 2387.

## References

1. Wang J., Neaton J.B., Zheng H. Epitaxial  $\text{BiFeO}_3$  multiferroic thin film heterostructures. *Science*. 2003, Vol. 299, P. 1719.
2. Zvezdin A. K., Pyatakov A. P. Phase transitions and the giant magnetoelectric effect in multiferroics. *Usp. Fiz. Nauk*. 2004, Vol. 174, Is. 4, P. 465.

3. Zvezdin A. K., Logginov A. S., Meshkov G. A. et al. Multiferroics: Promising materials for microelectronics, spintronics, and sensor technique. *Bull. Russ. Acad. Sci. Phys.* 2007, Vol. 71, P. 1561.
4. Aplesnin S. S. *Osnovi spintroniki* [Fundamentals of spintronics]. St. Petersburg, Lan Publ., 2022, 288 p.
5. Ennen I., Kappe D., Rempel T. et al. Giant Magnetoresistance: Basic Concepts, Microstructure, Magnetic Interactions and Applications. *Sensors.* 2016, Vol. 16, Is. 6, P. 904.
6. Binasch G., Grunberg P., Saurenbach F., Zinn W. Enhanced magnetoresistance in layered magnetic structures with antiferromagnetic interlayer exchange. *Phys. Rev. B.* 1989, Vol. 39, P. 4828.
7. Aplesnin S. S., Romanova O. B., Yanushkevich K. I. Magnetoresistance effect in anion-substituted manganese chalcogenides. *Phys. Stat. Sol. B Basic Research.* 2015, Vol. 252, Is. 8, P. 1792.
8. Aplesnin S. S., Sitnikov M. N., Romanova O. B. et al. Magnetoelectric and magnetoresistive properties of the  $\text{Ce}_x\text{Mn}_{1-x}\text{S}$  semiconductors. *Phys. Stat. Sol. B Basic Research.* 2016, Vol. 253, Is. 9, P. 1771.
9. Romanova O. B., Aplesnin S. S., Sitnikov M. N. et al. Magnetoresistance and magnetoimpedance in holmium manganese sulfides. *Appl. Phys. A.* 2022, Vol. 128, P. 124.
10. Zhang J. H., Zheng S. H., Tang Y. S. et al. Structural, magnetic, and dielectric properties of charge-order phases in manganite  $\text{La}(\text{Ca}_{0.8}\text{Sr}_{0.2})_2\text{Mn}_2\text{O}_7$ . *J. Appl. Phys.* 2020, Vol. 127, P. 104301.
11. Papavassiliou J. The Pinch Technique at Two Loops. *Phys. Rev. Lett.* 2000, Vol. 84, P. 2782.
12. Allodi G., De Renzi R., Guidi G. et al. Electronic phase separation in lanthanum manganites: Evidence from  $^{55}\text{Mn}$  NMR. *Phys. Rev. B.* 1997, Vol. 56, P. 6036.
13. Hennion M., Moussa F., Biotteau G. et al. Liquidlike Spatial Distribution of Magnetic Droplets Revealed by Neutron Scattering in  $\text{La}_{1-x}\text{Ca}_x\text{MnO}_3$ . *Phys. Rev. Lett.* 1998, Vol. 81, P. 1957.
14. Wang W., Li J., Liang Z. et al. Verwey transition as evolution from electronic nematicity to trimerons via electron-phonon coupling. *Sci. Adv.* 2023, Vol. 9, P. 8220.
15. Aplesnin S. S., Ryabinkina L. I., Abramova G. M. et al. Spin-dependent transport in  $\alpha$ -MnS single crystals. *Phys. Sol. St.* 2004, Vol. 46, Is. 11, P. 2067.
16. Aplesnin S. S., Ryabinkina L. I., Abramova G. M. et al. Conductivity, weak ferromagnetism, and charge instability in an  $\alpha$ -MnS single crystal. *Phys. Rev. B.* 2005, Vol. 71, Is. 12, P. 125204.
17. Wang S., Zhang J., Gharbi O. et al. Electrochemical impedance spectroscopy. *Nat. Rev. Meth. Prim.* 2021, Vol. 1, P. 41.
18. Holm S. Time domain characterization of the Cole-Cole dielectric model. *J. Electr. Bioimpedance.* 2020, Vol. 11, Is. 1, P. 101.
19. Parish M. M., Littlewood P. B. Magnetocapacitance in Nonmagnetic Composite Media. *Phys. Rev. Lett.* 2008, Vol. 101, P. 166602.
20. Yang Y.-F., Held K. Localization of strongly correlated electrons as Jahn-Teller polarons in manganites. *Phys. Rev. B.* 2007, Vol. 76, P. 212401.
21. Merten S., Shapoval O., Damaschke B. et al. Magnetic-field-induced suppression of Jahn-Teller phonon bands in  $(\text{La}_{0.6}\text{Pr}_{0.4})_{0.7}\text{Ca}_{0.3}\text{MnO}_3$ : the mechanism of colossal magnetoresistance shown by Raman spectroscopy. *Sci. Rep.* 2019, Vol. 9, P. 2387.

**Харьков Антон Михайлович** – кандидат физико-математических наук, доцент кафедры физики; Сибирский государственный университет науки и технологий имени академика М. Ф. Решетнева. E-mail: khark.anton@mail.ru.

**Ситников Максим Николаевич** – кандидат физико-математических наук, доцент кафедры физики; Сибирский государственный университет науки и технологий имени академика М. Ф. Решетнева. E-mail: kineru@mail.ru.

**Апленчин Сергей Степанович** – доктор физико-математических наук, профессор, заведующий кафедрой физики; Сибирский государственный университет науки и технологий имени академика М. Ф. Решетнева. E-mail: aplesnin@sibsau.ru.

**Kharkov Anton Mikhailovich** – Cand. Sc., Associate Professor of the Department of Physics; Reshetnev Siberian State University of Science and Technology. E-mail: khark.anton@mail.ru.

**Sitnikov Maksim Nikolaevich** – Cand. Sc., Associate Professor of the Department of Physics; Reshetnev Siberian State University of Science and Technology. E-mail: kineru@mail.ru.

**Aplesnin Sergey Stepanovich** – Dr. Sc., Professor, Head of the Department of Physics; Reshetnev Siberian State University of Science and Technology. E-mail: aplesnin@sibsau.ru.

---